Desalination and Water Treatment
www.deswater.com
doi: 10.1080/19443994.2014.893207

54 (2015) 1969–1980
May

Taylor & Francis
Taylor & Francis Group

Adsorption characteristics of dibutyl phthalate from aqueous solution using ginkgo leaves-activated carbon by chemical activation with zinc chloride

Zheng Wang*, Lei Chen

School of Civil Engineering, Nanjing Forestry University, Longpan Road 159#, Nanjing 210037, P.R. China
Tel. +86 025 85427691; email: wangzheng@njfu.edu.cn

Received 27 August 2013; Accepted 6 February 2014

ABSTRACT

The adsorption of dibutyl phthalate (DBP) from aqueous solution in batch experiments using ginkgo leaves-activated carbon (GLAC) by chemical activation with zinc chloride was investigated. After the activated carbon was characterized by scanning electron microscopy, energy-dispersive X-ray spectrometry, Brunauer–Emmett–Teller and Fourier transform infrared spectra, the influence of solution pH, adsorbent dosage, contact time, initial DBP concentration and temperature on the adsorption rate was investigated. The isotherm, kinetic and thermodynamic parameters were used to describe the experimental data. The maximum DBP adsorption rate was 97.46% at a pH of 13. Increase in GLAC dosage resulted in an increase in the removal of DBP. The adsorption percentage of DBP increased with increased contact time. The monolayer sorption capacity of the biosorbent for DBP was determined to be 129.87 mg/g with the Langmuir isotherm. The equilibrium data fitted better with the Freundlich isotherm than the Langmuir and D–R isotherms. The kinetic data were best described by the pseudo-second-order model. The thermodynamic studies indicated that the sorption process was thermodynamically feasible and spontaneous. Taking into consideration the above results, it can be concluded that the GLAC can be an alternative material for more costly adsorbents used for the removal of DBP in wastewater treatment processes.

Keywords: Adsorption characteristics; Dibutyl phthalate (DBP); Ginkgo leaves-activated carbon (GLAC); Activation; Zinc chloride

1. Introduction

Phthalates are non-halogenated esters of phthalic acid that find widespread utilization in various industrial and consumer-orientated applications. Less significant phthalate applications include components of adhesive materials, inks, materials for treating surfaces, lacquers, sealing and packing materials, solvents and fixing agents in fragrances, as well as additives in other kinds of cosmetics. The worldwide production of phthalic acid esters (PAEs) is approximately six million tons per year [1]. PAEs are not acutely toxic, but exposure over a reasonable period may result in potential carcinogenic effects and an unfavourable influence on the hormonal and reproductive system owing to their lipophilic properties.

*Corresponding author.

Studies have reported the occurrence of phthalate metabolites in urine specimens indicating the widespread exposure of humans to phthalates [2]. Nowadays, the types of PAEs that are controlled in the world are not chemically bound in a polymeric matrix but are gradually released during usage. They are controlled under the strictest supervision as they are regarded as the most problematic from the viewpoint of having undesirable effects on health. They include dibutyl phthalate (DBP), di (2-ethylhexyl) phthalate, diethyl phthalate, dimethyl phthalate, di-isononyl phthalate, butyl benzyl phthalate, di-isodecyl phthalate and di-n-octyl phthalate [3].

The most frequently detected type of PAE was reported to be DBP, in recent years among endocrine disrupting chemicals. Worldwide production of DBP is over 1 million tons per year. Humans can be simultaneously exposed to DBP through various routes, such as the intake of contaminated water. A prior research study tested water samples from the Chongqing section of the Jialing and Yangtze Rivers, and found high concentrations of DBP in many samples [4]. A study found DPB to be at the highest levels in venous blood followed by breast milk, umbilical cord blood and urine; this order depends on metabolic factors [5]. Another study found that women of childbearing age, 20–40 years old, are targets for the teratogenic effects of DBP [6]. As a reference index of the Standards for Drinking Water Quality of China (GB5749-2006), the limit of DBP is 3 μg/L [7]. The development of a sensitive and reliable method is necessary to remove DBP from resource water or treated drinking water, taking into account all of these considerations.

Past studies have reported a number of methods for removing PAEs from aqueous solutions. One of the most frequently applied methods is microbial degradation [8–10]. Other methods of PAE removal involve advanced oxidation processes (AOP) [11,12]. From these research conclusions on the treatment of PAEs, we find that DBP is not amenable to biological treatment due to its outstanding stability against microbial attack, and AOP are generally expensive. Hence, it is important to identify a method that is both effective and economical. Adsorption techniques are much preferred for the removal of PAEs because of their efficiency and low cost [13]. A whole range of adsorptive materials may be utilized for the adsorption of PAEs. Compared with other adsorbents used for DBP removal, activated carbon is considered as one of the most efficient and easy method to obtain as it is used in a wide range of applications in many fields and because it is made from many diverse raw materials [14,15].

The adsorption capacity of activated carbon depends on various factors such as surface area, pore size distribution and the surface functional groups of the adsorbent; polarity, solubility and molecule size of adsorbate; pH of solution, the presence of other ions in solution and so on [16]. The methods of activation commonly employed can broadly be divided into two main types: thermal (or physical) activation and chemical activation. Thermal activation involves primary carbonization (below 700˚C) followed by controlled gasification under the action of oxidizing gases at high temperatures (up to 1,100 ˚C). In chemical activation, the precursor is mixed with a chemical, restricting the formation of tars ($ZnCl_2$, H_3PO_4, etc.), after kneading it is carbonized and washed to produce the final activated carbon [17]. Both naturally occurring and synthetic carbonaceous materials have been used as precursors. Though new synthetic precursors such as polymeric fibers and phenolic-resin have been reported to produce activated carbon with high surface area, in recent years, industrial and agricultural by-products are increasingly being investigated as precursors [18,19].

The waste leaves of Casurina equisetifolia have been used as a low-cost source material for the preparation of activated carbons, and the carbons have been successfully used for adsorption of chromium from aqueous solution [20]. Gingko is a widely planted landscape tree species, with a huge quantity in many cities of China spread over 200,000 ha. There is a large available and inexpensive supply of over 120,000 tons of fallen ginkgo leaves. These leaves have no present commercial usage and are not eaten by livestock. There are no previous published reports on the use of activated carbon manufactured with ginkgo leaves for removing DBP from aqueous solution. Thus, ginkgo leaves, as a low-cost and abundant biomass resource, could be an alternative for the removal of DBP from wastewater or treated drinking water, greatly reducing the cost of DBP treatment.

The main objective of this research was to investigate the feasibility of using ginkgo leaves as a biomass resource for low-cost activated carbon and the removal characteristics of DBP from aqueous solution. After scanning electron microscopy (SEM), energy-dispersive X-ray spectrometry (EDS), Brunauer–Emmett–Teller (BET) and fourier transform infrared spectra (FTIR) characterization of this activated carbon by chemical activation with zinc chloride, the influences of different parameters including solution pH, GLAC dosage, contact time, DBP concentration and temperature were investigated. Additionally, the

isotherm, kinetic and thermodynamic parameters were explored to describe the experimental data.

2. Materials and methods

2.1. Activated carbon sample preparation and characterization

Samples of ginkgo leaves were obtained from the campus of Nanjing Forestry University, China. The samples were washed using distilled water and dried in a muffle heater at 60°C for 24 h. A longer drying time did not show an observable change in the sample weight. This was done to remove any adsorbed material in the raw sample to ensure adequate distribution and intercalation of chemicals in the next step. Then, the dried samples were pulverized to pass through 50 mesh sieves of diameter 355 μm [21,22]. The sample powder was stored in plastic bags for further tests to obtain char and activated carbon. Weighed samples were carbonized in the muffle furnace under a nitrogen atmosphere. The chemical-impregnated samples were subjected to a two-stage activation. First, 25 g of ginkgo leaves powder was immersed in 100 g of aqueous solution of chemical agent zinc chloride (25 wt.%) at room temperature for 5 h [21,22]. Second, the temperature was increased to 80°C at a heating rate of 5°C/min. The sample was exposed to this temperature for 3 h. It was then cooled to ambient temperature and left at rest for 16 h. The heating rate and duration were considered adequate for complete distribution and intercalation of the chemicals in the sample matrix [21,22]. After the treatment, the samples were filtered to remove excess chemicals from the solution. Then they were dried at 105°C for 24 h to ensure complete removal of water, while leaving the chemicals in the samples. For the carbonization, the samples were heated at 5°C/min to 100°C and held for 1 h. This was to remove adsorbed water and volatile matter. Then the temperature was increased in steps of 15 °C/min to the desired temperature 600°C, which was held constant for 2 h. Then the sample was cooled to ambient temperature. The carbonization was done under flow of nitrogen (500 mL/min). The prepared activated carbon was thoroughly washed with distilled water until a neutral pH was obtained [21,22].

The BET surface area and total pore volume of the activated carbon sample were determined using a surface analyser (Autosorb-1C, Quantachrome Instrument, USA). Nitrogen was used as cold bath (77.35 K). An FTIR spectrometer (model 360, Thermo Nicolet Instrument, USA) was employed to determine the presence of functional groups in all the adsorbents at room temperature. A pellet (pressed-disk) technique was used for this purpose. The pellets were prepared by mixing the adsorbent with KBr (mass ratio 100:1). The spectral range covered was 4,000 to 500 cm^{-1}; scanning was performed at a rate of 16 nm s^{-1}. A scanning electron microscope (model S-3400 N II, Hitachi Instrument, Japan) was used to obtain SEM micrographs of the activated carbon. Samples of activated carbon were all gold plated and an electron acceleration voltage of 20 kV was applied for SEM observation. The predominant elements of ginkgo leaves-activated carbon and raw resources were analysed using an EDS (model EX-250, Horiba Instrument, Japan).

2.2. Adsorbate and analytical measurements

A stock DBP solution of 1,000 mg/L was prepared from DBP (99% purity, $C_{16}H_{22}O_4$, FW: 278.34, AccuStandard Inc., USA) dissolved in methanol. The working solutions with different concentrations were prepared by appropriate dilutions of the stock solution. The concentration of DBP in aqueous solution was analysed by a high-performance liquid chromatography (HPLC, model LaChrom Elite L-2000, Hitachi Instrument, Japan) using a Hitachi LaChrom C18 (5 μm) 4.6 mm I.D. × 150 mm separation column at a wavelength of 202 nm. The mobile phase was a mixture of water and methanol (10:90, v/v), and the flow rate was 1.0 mL·min^{-1}. The injection volume was 10 μL, and the column temperature was 30°C. Under this chromatographic condition, the baseline separation for DBP could be obtained within 15 min [23]. A digital pH metre (model: PHS-3C: PSI Co. Ltd., Shanghai, China) was used for pH measurement.

2.3. Batch adsorption experiments

A typical adsorption experiment was conducted by using the necessary GLAC in a 250 mL stopper conical flask at desired pH value, contact time, temperature and DBP concentration. The pH values of the solution were adjusted by adding negligible volumes of 0.1 M HCl or NaOH. The flask was shaken for the desired contact time in a rotary shaker fixed at 150 rpm. The contents of the flask were filtered through a 0.45 μm filter membrane, and the filtrate was analysed for the remaining DBP concentration. The removal percentage of DBP was determined from the initial and final concentrations of DBP in the liquid phases. The pH of the solutions was checked before the beginning and at the end of the adsorption experiments. The adsorption experiment was conducted three times for each

sample, and each individual chemical assay was conducted in duplicate.

The percentage of DBP adsorption by the GLAC was computed using the equation:

$$\text{Adsorption percentage, } \% = \frac{C_0 - C_t}{C_0} \times 100 \quad (1)$$

where C_0 and C_t are the concentrations of DBP (mg/L) in the solution at initial and at time t (min). Adsorption capacity was calculated by using the mass balance equation for the adsorbent:

$$q = \frac{(C_0 - C_e)V}{M} \quad (2)$$

where q is the adsorption capacity (mg/g) and C_e is the equilibrium concentration of DBP (mg/L) in the solution. V is the volume of DBP solution (L), and M is the weight of GLAC (g).

The effect of pH on DBP removal was investigated in the initial pH range of 1–13. Adsorption experiments for the effect of pH were conducted by using a 100 mL DBP solution having a concentration of 5 mg/L with a GLAC dosage of 0.1 g/L for a contact time of 2 h at 298 K. The effect of GLAC dosage level on percent removal of DBP was studied using a 100 mL DBP solution having a concentration of 5 mg/L. The selected GLAC was used at dosages ranging from 0.1 to 1 g/L for a contact time of 2 h at 298 K. The effect on the variation of the initial concentration of the solution was studied using a 100 mL DBP solution of varying concentrations (5–15 mg/L), a contact time of 2 h and a GLAC dosage level of 0.1 g/L at 298 K. Kinetics analysis for the adsorption process was studied on the batch adsorption of a 100 mL DBP solution having concentration of 5 mg/L with a GLAC dosage of 0.1 g/L. The contact time was varied from 20 to 120 min at 298 K. The effect of temperature was evaluated using a 100 mL DBP solution with a concentration of 5 mg/L with a GLAC dosage of 0.1 g/L for a contact time of 2 h. The selected temperatures ranged from 298 to 308 K.

3. Results and discussion

3.1. Characterization of the GLAC

3.1.1. SEM micrographs

The SEM micrographs are shown in Fig. 1 for ginkgo leaves powder and GLAC at 500 and 5,000 times magnification. It is seen from Fig. 1(a) and (b) that the surface texture of the ginkgo leaves is fibrous. From Fig. 1(c) and (d), we can see that the micromorphology of the GLAC change largely when ginkgo leaves have finished the carbonization process. Porous structures in a honeycomb shape were clearly observed on the GLAC surface, crevices and skeletal structure are at other places. Activated carbon is generally described as an amorphous form of graphite with a random structure of graphite plates having a highly porous structure with a range of cracks and crevices reaching molecular dimensions [13].

3.1.2. EDS analysis

The EDS analysis of ginkgo leaves powder and GLAC is indicated in Fig. 2. The conclusions from the EDS analysis are enumerated in Table 1. From Table 1, it was seen that the main elements of ginkgo leaves were 62.34% carbon and 34.29% oxygen; after carbonization, they were 78.21 and 12.6%, respectively. Due to the use of zinc chloride as an activator, the elements zinc and chloride increased from 0 and 0.12 to 4.69% and 3.12% after carbonization, respectively. The other elements of ginkgo leaves powder and GLAC changed little.

3.1.3. Surface area and pore structure characterization

The specific surface area and pore structure of GLAC were analysed based on the nitrogen adsorption at 77.35 K. The BET surface area of the sample was 696.58 m^2/g. The single point total pore volume was found to be 0.59 cm^3/g with an average pore diameter of 5.76 nm. Pore sizes are classified in accordance with the classification adopted by the International Union of Pure and Applied Chemistry, that is, micropores (diameter (d) < 2 nm), mesopores (2 nm < d < 50 nm) and macropores (d > 50 nm) [24,25]. The results of analysis suggested that the GLAC contains a relatively high surface area and total pore volume. The analysis of the adsorbent showed the predominance of a microporous structure.

3.1.4. FTIR analysis

The FTIR is an important technique to determine characteristic functional groups, which make the adsorption behaviour possible [26]. The infrared spectrum of ginkgo leaves powder and GLAC are presented in Fig. 3 and Table 2. As shown in Fig. 3, the infrared spectrum showed a large number of adsorption peaks, which suggested the complexity of the

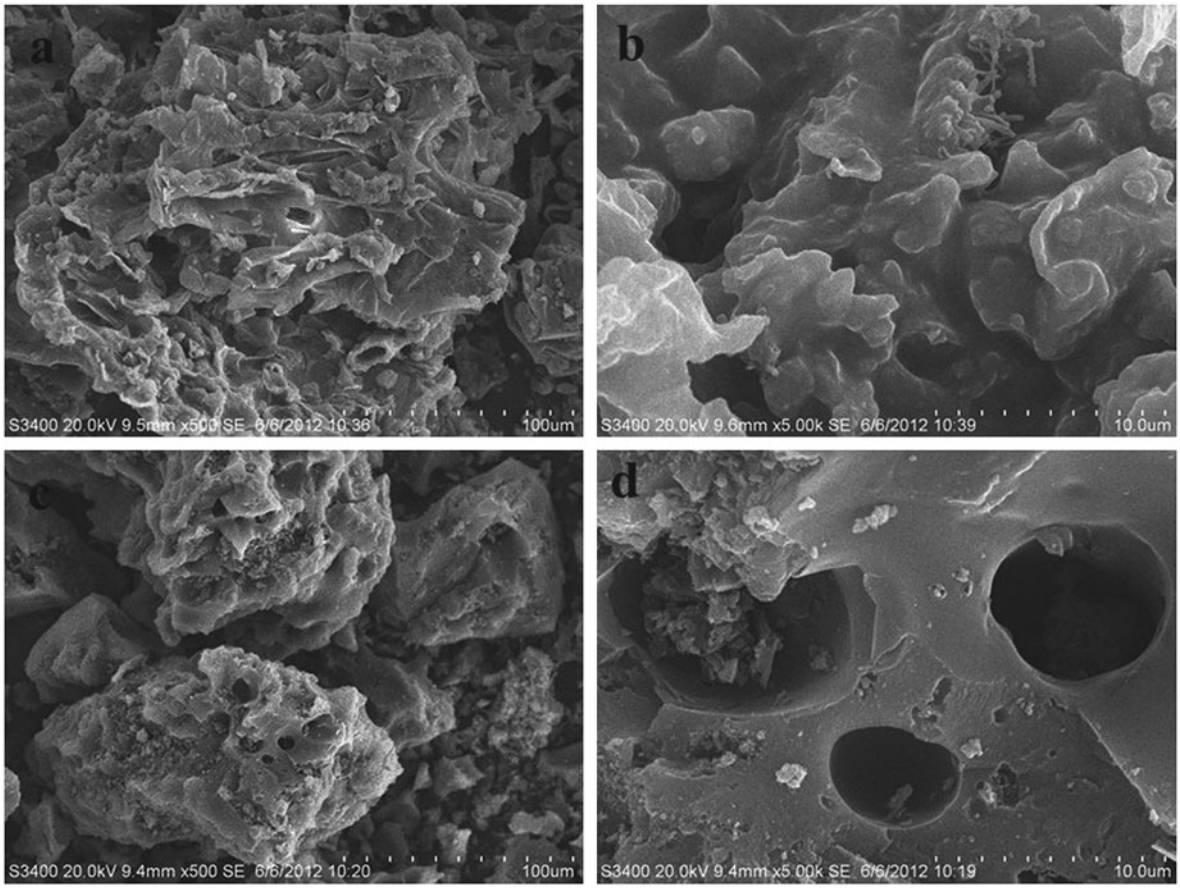

Fig. 1. SEM photographs of ginkgo leaves powder at (a) ×500 and (b) ×5,000 magnification and GLAC at (c) ×500 and (d) ×5,000 magnification.

material. There were strong peaks at 3,451 and 3,452 cm^{-1} of ginkgo leaves powder and GLAC representing the OH stretching of the phenol group, and the peaks at 2,932 and 2,930 cm^{-1}, indicate the presence of CH_2 stretching. The appearance of peaks of ginkgo leaves powder and GLAC at 2,873 and 2,870 cm^{-1} indicate the presence of CH_3 stretching. The adsorption peak of ginkgo leaves powder at 1,793 cm^{-1} was attributed to C=O stretching. The peaks of ginkgo leaves powder and GLAC at 1,643 and 1,650 cm^{-1} showed the C=C stretching. The peak of ginkgo leaves powder at 1,459 cm^{-1} was associated with the existence of CH_2 deformation. The adsorption peaks of ginkgo leaves powder and GLAC were observed at approximately 1,399 and 1,402 cm^{-1} could be attributed to N–H stretching. The peak of ginkgo leaves powder at 1,322 cm^{-1} indicate N–H stretching as well. The bonds near 1,129 and 1,132 cm^{-1} indicate the existence of C=O stretching. Peaks at 1,078 cm^{-1} and 1,073 cm^{-1} in the FTIR spectrum of ginkgo leaves powder and GLAC may be due to six-member cyclic ether. The peaks of ginkgo leaves powder at 791 and 679 cm^{-1} were assigned to Si–O stretching and P-OH stretching, respectively [24–28]. These observations and conclusions regarding the spectrum indicate the possible involvement of those functional groups on the surface of GLAC during the adsorption process.

3.2. Effect of solution pH

The pH of the solution is an important variable affecting the adsorption characteristics. Change of the adsorption capacity of DBP on GLAC with pH was shown in Fig. 4. From Fig. 4, the maximum adsorption rate was 97.46%, and the maximum adsorption capacity was 48.73 mg/g at a pH of 13. The minimum adsorption rate was 70.97%, and the minimum adsorption capacity was 35.49 mg/g at a pH of 7. The adsorption rate of DBP had little change, with an average adsorption rate of 74.35% and an average adsorption capacity 37.18 mg/g when the pH of the solution was adjusted from 1 to 9, indicating that

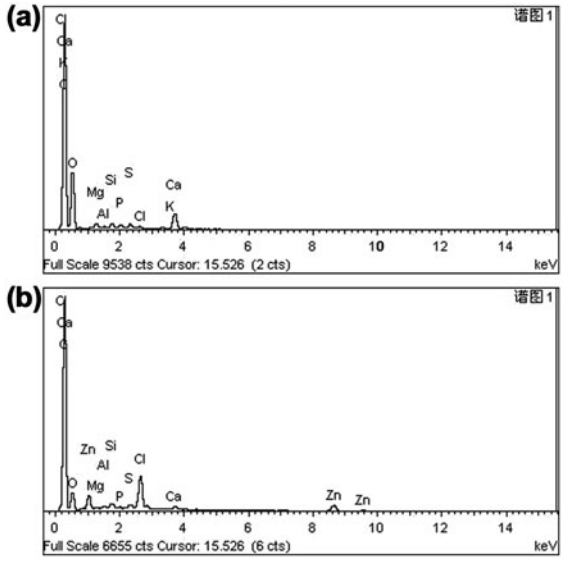

Fig. 2. EDS of (a) ginkgo leaves powder and (b) GLAC.

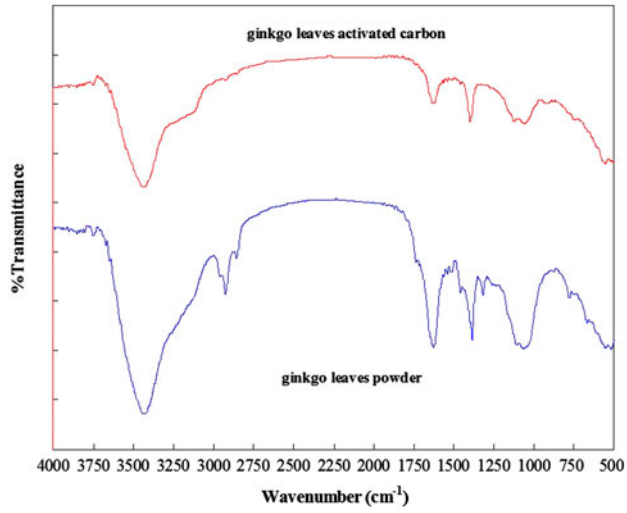

Fig. 3. FTIR spectra recorded for ginkgo leaves powder and GLAC.

Table 1
EDS analysis conclusions of ginkgo leaves powder and GLAC

Element	Ginkgo leaves powder, wt.%	GLAC, wt.%
C	62.34	78.24
O	34.29	12.60
Mg	0.36	0.10
Al	0.06	0.19
Si	0.26	0.35
P	0.25	0.09
S	0.29	0.30
Cl	0.12	3.12
K	0.13	–
Ca	1.90	0.32
Zn	–	4.69
Totals	100.00	100.00

the electrostatic mechanism was not the only mechanism for DBP adsorption in the present system. Adsorption capacity was also affected by the chemical reaction between the GLAC and the DBP. As the solution pH increased from 9 to 13, the number of positively charged surface sites on the adsorbent increased, which may result in the increase in adsorption of DBP molecules due to the electrostatic attraction [24]. However, it did not explain the slight changes of the DBP adsorption at acidic, neutral and weak alkaline solution conditions [25].

Table 2
FTIR of ginkgo leaves powder and GLAC

S. no.	Frequency (cm^{-1}) of ginkgo leaves powder	Frequency (cm^{-1}) of GLAC	Differences	Assignment
1	3,451	3,452	1	OH stretching
2	2,932	2,930	−1	CH_2 stretching
3	2,873	2,870	−3	CH_3 stretching
4	1,739	–	–	C=O stretching
5	1,643	1,650	7	C=C stretching
6	1,459	–	–	CH_2 deformation
7	1,399	1,402	3	N–H stretching
8	1,322	–	–	N–H stretching
9	1,129	1,132	3	C=O stretching
10	1,078	1,073	−5	Six member cyclic ether
11	791	–	–	Si–O stretching
12	679	–	–	P–OH stretching

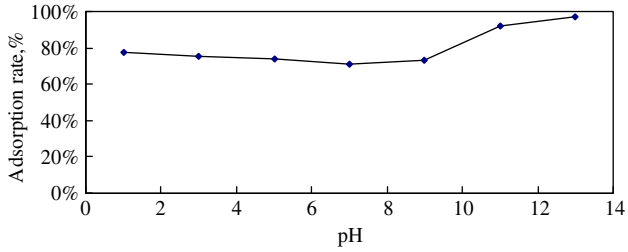

Fig. 4. Effect of pH on DBP adsorption by GLAC.

3.3. Effect of initial GLAC dosage

The effect of GLAC dosage on DBP adsorption is depicted in Fig. 5. Increase in GLAC dosage resulted in an increase in the removal of DBP; the percentage of DBP adsorption increased from 68.56 to 98.42% with an increase in adsorbent mass from 0.01 to 0.1 g; however, the adsorption capacity decreased from 34.28 to 4.92 mg/g. The percentage removal increased with the GLAC dosage up to a certain limit, after which a constant value was reached. The increase in adsorption of DBP with adsorbent dosage can be attributed to increased surface area and the availability of more adsorption sites [25]. The adsorption capacity was lesser at higher adsorbent doses. This was due to greater availability of the exchangeable sites or surface area at a higher concentration of the adsorbent [26].

3.4. Effect of contact time

The effect of contact time on the adsorption of DBP by GLAC is shown in Fig. 6, where is it illustrated that the adsorption percentage of DBP increased with the increase of contact time. The adsorption of DBP on GLAC was found to be rapid at the initial period and then becomes slow and stagnates with an increase in contact time. The adsorption rate of DBP was 32% and the adsorption capacity was 16 mg/g through 20 min adsorption. The time required to reaching adsorption equilibrium between

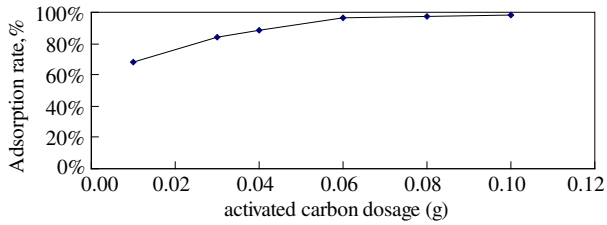

Fig. 5. Effect of initial GLAC dosage on DBP adsorption.

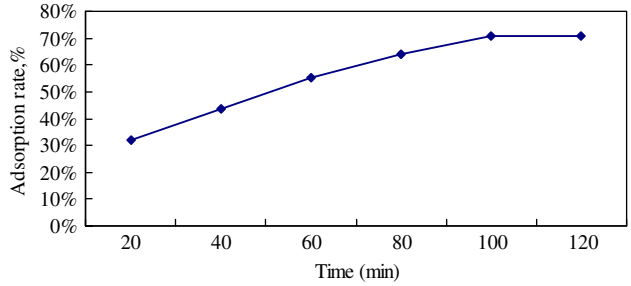

Fig. 6. Effect of contact time on DBP adsorption.

the adsorbent and the DBP solution was less than 100 min with an adsorption rate 70.75% and an adsorption capacity 35.38 mg/g. The steep slope of DBP adsorption indicated instantaneous adsorption which might be due to the effect of surface acidic functional groups on the surface of adsorbent [27]. Therefore, the adsorption of DBP was thought to have probably taken place via surface adsorption until the surface functional sites were fully occupied; thereafter, DBP molecules diffuse into the pores of the adsorbent for further adsorption. Thus, it was assumed that longer treatment might not have further effect to change the property of the adsorbent.

3.5. Adsorption isotherm

For the solid–liquid adsorption system, the adsorption isotherm is an important model in the description of adsorption behaviour. When the adsorption reaction reaches an equilibrium state, the adsorption isotherm can indicate the distribution of adsorbate molecules between the solid phase and the liquid phase [24]. It is important to understand the adsorption behaviour to in order to identify the most appropriate adsorption isotherm model. In this study, the Langmuir, Freundlich and Dubinin–Radushkevich (D–R) isotherm models were employed to investigate the adsorption behaviour.

3.5.1. Langmuir model

This model assumes that the adsorptions occur at specific homogeneous sites on the adsorbent and are used successfully in many monolayer adsorption processes. The Langmuir-type adsorption isotherm indicates surface homogeneity of the adsorbent and hints towards the conclusion that the surface of the adsorbent is made up of small adsorption patches which are energetically equivalent to each other in respect to the adsorption phenomenon [25]. The Langmuir model is given by the following equation:

$$\frac{1}{q_e} = \frac{1}{q_m b C_e} + \frac{1}{q_{\max}} \quad (3)$$

where q_m shows the monolayer sorption capacity (mg/g), b is the Langmuir constant (L/mg), C_e is equilibrium dye concentration in the solution (mg/L) and q_e represents amounts of DBP adsorbed onto GLAC at equilibrium (mg/g). The plot of $1/q_e$ vs. $1/C_e$ was employed to generate the intercept value of $1/q_m$ and slope of $1/q_m b$ (Fig. 7).

Through the above calculation, q_m and b were determined to be 129.87 mg/g and 5.5 L/mg, respectively. The correlation coefficient (R^2) was 0.9615. One of the essential characteristics of the Langmuir model can be expressed in terms of the dimensionless constant separation factor for the equilibrium parameter R_L, defined as:

$$R_L = \frac{1}{1 + bC_0} \quad (4)$$

where C_0 is the maximum initial concentration of DBP (mg /L). The value of R_L indicates the type of isotherm to be irreversible ($R_L = 0$), favourable ($0 < R_L < 1$), linear ($R_L = 1$) or unfavourable ($R_L > 1$). The R_L value in the study was found to be 0.012, indicating that this sorption process is favourable [26].

3.5.2. Freundlich isotherm

The Freundlich isotherm is an empirical equation employed to describe heterogeneous surfaces systems [28]. The Freundlich equation is expressed as:

$$\ln q_e = \ln k_f + \frac{1}{n} \ln C_e \quad (5)$$

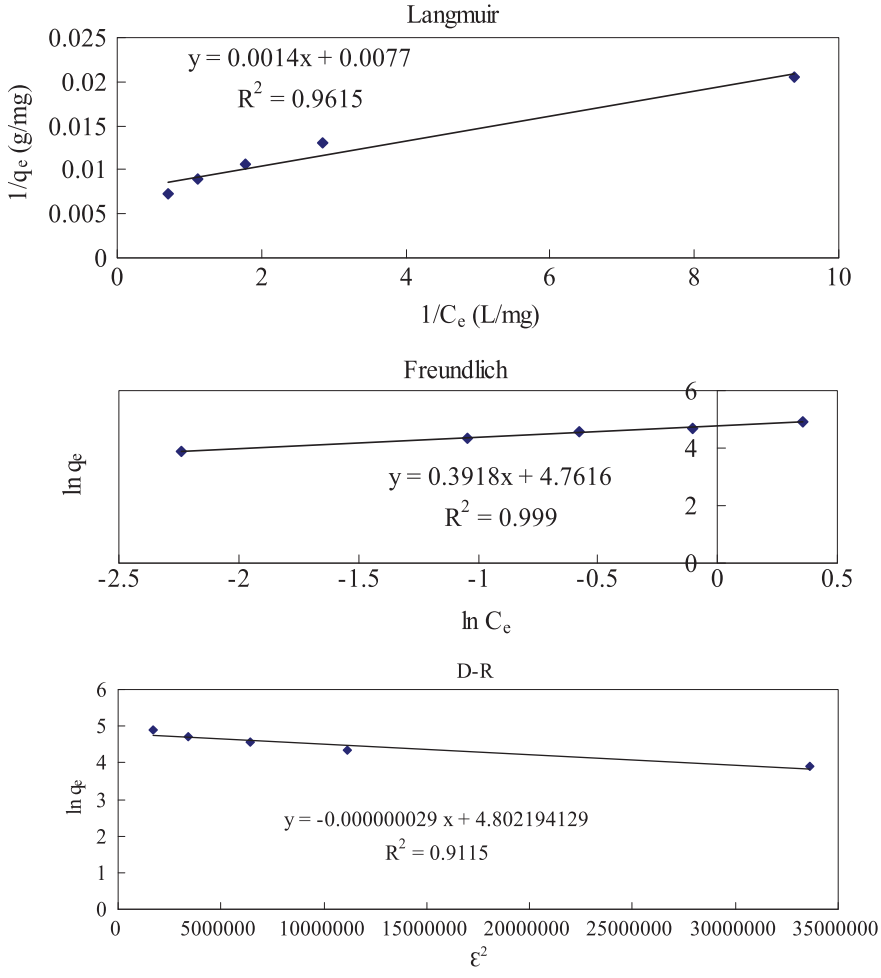

Fig. 7. The linear plots of Langmuir, Freundlich and D–R equilibrium models.

where k_f and $1/n$ are Freundlich constants, C_e is the equilibrium concentration of the solution (mg /L) and q_e is the equilibrium adsorption capacity per unit weight adsorbent (mg/g).

The equilibrium experimental data were fitted using the Freundlich isotherm, and the plot of non-linear form of Freundlich isotherm curves is presented in Fig. 7. The Freundlich parameters k_f, $1/n$ and R^2 evaluated from the non-linear plot using non-linear regressive analysis were 116.9, 0.3918 and 0.999, respectively. The Freundlich parameter $1/n$ relates to the surface heterogeneity. When $0 < 1/n < 1$, the adsorption is favourable; when $1/n = 1$, the adsorption is homogeneous and there is no interaction among the adsorbed species; and when $1/n > 1$, the adsorption is unfavourable [24]. In general, $1/n = 0.3918$ indicated that the adsorption behaviour of DBP on GLAC was carried out easily.

3.5.3. D–R isotherm

The D–R isotherm model is more general than the Langmuir isotherm, because it does not assume a homogeneous surface or constant sorption potential. The following equation indicates the D–R isotherm [22]:

$$\ln q_e = \ln q_m - B\varepsilon^2 \tag{6}$$

$$\varepsilon = RT \ln\left(1 + \frac{1}{C_e}\right) \tag{7}$$

where q_m is the theoretical saturation capacity (mg/g), B is a constant related to the sorption energy (M^2/kJ^2), ε is the Polanyi potential, R is the universal gas constant (8.314 J/ (M K)) and T is the absolute temperature (K). The values of q_m and B were obtained by plotting $\ln q_e$ vs. ε^2 as seen in Fig. 7. Through the above calculations, q_m and B were found to be 121.45 mg/g and 0.000000029 M^2/kJ^2, respectively. R^2 was determined to be 0.9115.

3.6. Kinetic studies

The kinetics of the adsorption process have been evaluated for this work. This study describes the solute uptake rate and evidently, this rate controls the residence time of adsorbate uptake at the solid–liquid interface including the diffusion process. The mechanism of adsorption depends on the physical and chemical characteristics of the adsorbents. In order to determinate the mechanism of DBP adsorbed on GLAC, several commonly used adsorption kinetics models were employed to discuss the controlling mechanism [25].

3.6.1. Pseudo-first-order model

The pseudo-first-order rate model from Lagergren [24] is based on solid capacity and is generally expressed as:

$$\frac{dq}{dt} = k_1 (q_e - q) \tag{8}$$

where q_e is the amount of solute adsorbed at equilibrium per unit weight of adsorbent (mg/g), q is the amount of solute adsorbed at any time (mg/g) and k_1 is the pseudo-first-order rate constant (min^{-1}). Eq. (8) is integrated for the boundary conditions $t = 0$ to $t > 0$ ($q = 0$ to $q > 0$) and then rearranged to obtain the following linear time-dependent function:

$$\ln(q_e - q) = \ln q_e - k_1 t \tag{9}$$

This is the most popular form of the pseudo-first-order kinetic model. Fig. 8 shows an example for these plots. The constant k_1 and R^2 were calculated as 0.0177 and 0.9704, respectively.

3.6.2. Pseudo-second-order model

The kinetic data were further analysed using the pseudo-second-order model [25] which can be expressed as:

$$\frac{dq}{dt} = k_2 (q_e - q)^2 \tag{10}$$

Integrating Eq. (10) for the boundary conditions $t = 0$ to $t > 0$ and $q = 0$ to $q > 0$ and rearranging it to obtain the linearized form, shown as:

$$\frac{t}{q} = \frac{1}{k_2 q_e^2} + \frac{t}{q_e} \tag{11}$$

where k_2 is the pseudo-second-order rate constant (g/(mg min)). The plot of t/q vs. t of Eq. (11) should give a linear relationship, from which q_e and k_2 can be determined from the slope and intercept of the plot (Fig. 8). The constant k_2 and R^2 were calculated as 0.000432 and 0.9885, respectively.

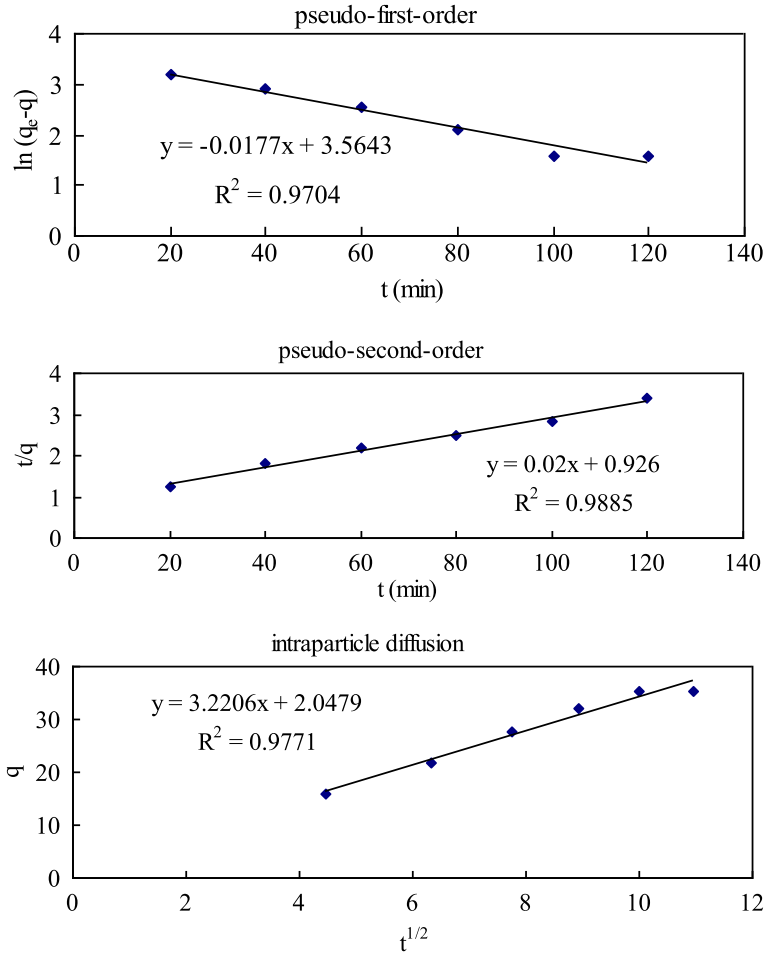

Fig. 8. The linear plots of pseudo-first-order kinetic, pseudo-second-order kinetic and intraparticle diffusion models.

3.6.3. Intraparticle diffusion model

The intraparticle diffusion model is used to explain the diffusion mechanism of the adsorption process. The equation is described in [24]:

$$q = k_t \times t^{1/2} + C \tag{12}$$

where k_t is the intraparticle diffusion rate constant (mg/(g min$^{1/2}$) and C is the intercept. The value of C relates to the thickness of the boundary layer. The larger C implies the greater effect of the boundary layer. According to Eq. (12), if the adsorption mechanism follows the intraparticle diffusion model, the plot of q vs. $t^{1/2}$ should result in a linear relationship (Fig. 8). The slope k_t and intercept C were 3.2206 and 2.0479, respectively, and were obtained by linear fitting analysis. The value of R^2 was 0.9771.

The R^2 value of the pseudo-second-order kinetic model for this model is higher than that of the pseudo-first-order kinetic and the intraparticle diffusion model. Hence, it can be assumed that the adsorption of DBP perfectly follows the pseudo-second-order kinetic model.

3.7. Thermodynamic studies

The temperature dependence of the equilibrium constant, K can be used to determine the thermodynamic parameters [29]. The Van't Hoff equation is used to evaluate the variation of the equilibrium constant with temperature. The integrated form of this equation is given as:

$$\ln K = \frac{\Delta S^\circ}{R} - \frac{\Delta H^\circ}{RT} \tag{13}$$

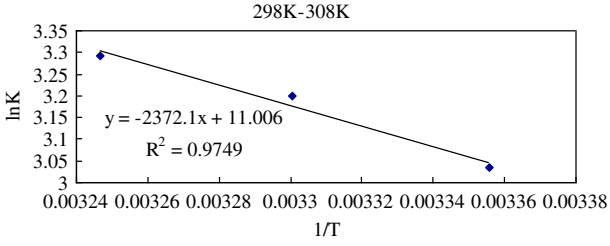

Fig. 9. The effect of temperature on the equilibrium distribution coefficient.

$$K = \frac{q_e \rho}{C_e} \tag{14}$$

where $\rho = 1{,}000\ \mathrm{kg/m^3}$ is the density of the solution mixture, ΔH° is the standard enthalpy change (J/M), ΔS° is the standard entropy change (J/M K), T is the absolute temperature (K) and K is the distribution coefficient. The ΔH° and ΔS° of the process can be determined from the slope and intercept of line obtained by plotting $\ln K$ vs. $1/T$. The Van't Hoff plot for DBP adsorption of GLAC is shown in Fig. 9. The ΔH° and ΔS° for DBP can be calculated from the slope of the straight line.

The Gibbs free energy change of adsorption (ΔG°) for each temperature is then obtained as [30]:

$$\Delta G^\circ = \Delta H^\circ - T\Delta S^\circ \tag{15}$$

From Eq. (15), ΔG° was calculated as –7.55, –8.00 and –8.46 kJ/M for the adsorption of DBP on GLAC at 298, 303 and 308 K, respectively. The negative ΔG° values indicate that the adsorption of DBP on GLAC was thermodynamically feasible and spontaneous [31]. The ΔH° and ΔS° were determined as 19.72 kJ/M and 91.5 J/(M K), respectively. The positive values of ΔH° indicated the endothermic nature of the process, whereas the positive ΔS° value confirmed the increased randomness at the solid-solute interface during adsorption and reflected the sorption of GLAC for DBP. The low value of ΔS° also indicated that no remarkable change on entropy occurs [31].

4. Conclusions

The present study shows that GLAC by chemical activation with zinc chloride can be used as an adsorbent for the removal of DBP from aqueous solutions. The main elements of GLAC are 78.21% carbon and 12.6% oxygen. The BET surface area of the sample is 696.58 $\mathrm{m^2/g}$ with an average pore diameter of 5.76 nm. The infrared spectrum showed the complexity of the material. The maximum DBP adsorption rate was 97.46%, and the maximum adsorption capacity was 48.73 mg/g at a pH of 13. Increase in GLAC dosage resulted in an increase in removal of DBP. The adsorption percentage of DBP increased with the increase of contact time. The monolayer sorption capacity of the biosorbent for DBP was found to be 129.87 mg/g with the Langmuir isotherm. The equilibrium data fitted with the Freundlich isotherm better than the Langmuir and D–R isotherms. The kinetic data were best described by the pseudo-second-order model. The thermodynamic studies indicated that the sorption process was thermodynamically feasible and spontaneous. It can be concluded that GLAC can be an alternative material for more costly adsorbents used for DBP removal in wastewater treatment processes.

Acknowledgements

The authors express their sincere gratitude to the Natural Science Foundation of the Jiangsu Higher Education Institutions of China (12KJB560004), the Housing and Urban and Rural Construction Technology Program of the Ministry of Science and Project (2011-K7-2), the project of Jiangsu government scholarship for study abroad (2012196) and a project funded by the Priority Academic Program Development of the Jiangsu Higher Education Institutions (PAPD) for financial support.

References

[1] M.M. Abdel Daiem, J. Rivera-Utrilla, R. Ocampo-Pérez, J.D. Méndez-Díaz, M. Sánchez-Polo, Environmental impact of phthalic acid esters and their removal from water and sediments by different technologies—A review, J. Environ. Manage. 109 (2012) 164–178.
[2] Y. Guo, Q. Wu, K. Kannan, Phthalate metabolites in urine from China, and implications for human exposures, Environ. Int. 37 (2011) 893–898.
[3] M. Julinová, R. Slavík, Removal of phthalates from aqueous solution by different adsorbents: A short review, J. Environ. Manage. 94 (2012) 13–24.
[4] S.J. Zheng, H.J. Tian, J. Cao, Y.Q. Gao, Exposure to di(n-butyl)phthalate and benzo(a)pyrene alters IL-1β secretion and subset expression of testicular macrophages, resulting in decreased testosterone production in rats, Toxicol. Appl. Pharm. 248 (2010) 28–37.
[5] J.A. Chen, H.J. Liu, Z.Q. Qiu, W.Q. Shu, Analysis of di-n-butyl phthalate and other organic pollutants in Chongqing women undergoing parturition, Environ. Pollut. 156 (2008) 849–853.

[6] Y.J. Zhu, J.T. Jiang, L. Ma, J. Zhang, Y. Hong, K. Liao, Q. Liu, G.H. Liu, Molecular and toxicologic research in newborn hypospadiac male rats following in utero exposure to di-n-butyl phthalate (DBP), Toxicology 260 (2009) 120–125.
[7] Health Ministry of People's Republic of China, Standards for drinking water quality of China (GB5749-2006), 2007.
[8] M.Z. Huang, Y.W. Ma, Y. Wang, J.Q. Wan, H.P. Zhang, The fate of di-n-butyl phthalate in a laboratory-scale anaerobic/anoxic/oxic wastewater treatment process, Bioresource Technol. 101 (2010) 7767–7772.
[9] J. Chi, Q. Yang, Effects of *Potamogeton crispus* L. on the fate of phthalic acid esters in an aquatic microcosm, Water Res. 46 (2012) 2570–2578.
[10] B.V. Chang, Y.S. Lu, S.Y. Yuan, T.M. Tsao, M.K. Wang, Biodegradation of phthalate esters in compost-amended soil, Chemosphere 74 (2009) 873–877.
[11] S. Kaneco, H. Katsumata, T. Suzuki, K. Ohta, Titanium dioxide mediated photocatalytic degradation of dibutyl phthalate in aqueous solution-kinetics, mineralization and reaction mechanism, Chem. Eng. J. 125 (2006) 59–66.
[12] L.S. Li, W.P. Zhu, L. Chen, P.Y. Zhang, Z.Y. Chen, Photocatalytic ozonation of dibutyl phthalate over TiO_2 film, J. Photoch. Photobiol. A: Chem. 175 (2005) 172–177.
[13] Z.Q. Fang, H.J. Huang, Adsorption of di-n-butyl phthalate onto nutshell-based activated carbon. Equilibrium, kinetics and thermodynamics, Adsorpt. Sci. Technol. 27(7) (2009) 685–700.
[14] F. Wang, J. Yao, K. Sun, B.S. Xing, Adsorption of dialkyl phthalate esters on carbon nanotubes, Environ. Sci. Technol. 44 (2010) 6985–6991.
[15] C.Y. Chen, C.C. Chen, Y.C. Chung, Removal of phthalate esters by α-cyclodextrin-linked chitosan bead, Bioresource Technol. 98 (2007) 2578–2583.
[16] E. Lorenc-Grabowska, G. Gryglewicz, Adsorption characteristics of Congo Red on coal-based mesoporous activated carbon, Dyes Pigments 74 (2007) 34–40.
[17] A.A. Ahmad, B.H. Hameed, Fixed-bed adsorption of reactive azo dye onto granular activated carbon prepared from waste, J. Hazard. Mater. 175 (2010) 298–303.
[18] A.P. Carvalho, B. Cardoso, J. Pires, M. Brotas de Carvalho, Preparation of activated carbons from cork waste by chemical activation with KOH, Carbon 41 (2003) 2873–2876.
[19] F. Suárez-García, A. Martínez-Alonso, J.M.D. Tascón, Activated carbon fibers from Nomex by chemical activation with phosphoric acid, Carbon 42(8–9) (2004) 1419–1426.
[20] K. Ranganathan, Chromium removal by activated carbons prepared from Casurina equisetifolia leaves, Bioresource Technol. 73 (2000) 99–103.
[21] B. Jibril, O. Houache, R. Al-Maamari, B. Al-Rashidi, Effects of H_3PO_4 and KOH in carbonization of lignocellulosic material, J. Anal. Appl. Pyrolysis 83 (2008) 151–156.
[22] Z.Z. Li, X.W. Tang, Y.M. Chen, L.M. Wei, Y. Wang, Activation of Firmiana Simplex leaf and the enhanced Pb(II) adsorption performance: Equilibrium and kinetic studies, J. Hazard. Mater. 169 (2009) 386–394.
[23] Y.M. Ren, Q. Dong, J. Feng, J. Ma, Q. Wen, M.L. Zhang, Magnetic porous ferrospinel $NiFe_2O_4$: A novel ozonation catalyst with strong catalytic property for degradation of di-n-butyl phthalate and convenient separation from water, J. Colloid Interf. Sci. 382 (2012) 90–96.
[24] X.L. Han, W. Wang, X.J. Ma, Adsorption characteristics of methylene blue onto low cost biomass material lotus leaf, Chem. Eng. J. 171 (2011) 1–8.
[25] A. Ahmad, M. Rafatullah, O. Sulaiman, M.H. Ibrahim, R. Hashim, Scavenging behaviour of meranti sawdust in the removal of methylene blue from aqueous solution, J. Hazard. Mater. 170 (2009) 357–365.
[26] G.O. El-Sayed, Removal of methylene blue and crystal violet from aqueous solutions by palm kernel fiber, Desalination 272 (2011) 225–232.
[27] H. Deng, J.J. Lu, G.X. Li, G.L. Zhang, X.G. Wang, Adsorption of methylene blue on adsorbent materials produced from cotton stalk, Chem. Eng. J. 172 (2011) 326–334.
[28] H.A. AL-Aoh, M.J. Maah, A.A. Ahmad, M.R. Abas, Adsorption of 4-nitrophenol on palm oil fuel ash activated by amino silane coupling agent, Desalin. Water Treat. 40 (2012) 159–167.
[29] A. Kumar, B. Prasad, I.M. Mishra, Adsorptive removal of acrylonitrile by commercial grade activated carbon: Kinetics, equilibrium and thermodynamics, J. Hazard. Mater. 152 (2008) 589–600.
[30] A. Omri, M. Benzina, Adsorption characteristics of silver ions onto activated carbon prepared from almond shell, Desalin. Water Treat. 51 (2013) 2317–2326.
[31] Z.W. Wang, P. Han, Y.B. Jiao, D. Ma, C.C. Dou, R.P. Han, Adsorption of congo red using ethylenediamine modified wheat straw, Desalin. Water Treat. 30 (2011) 195–206.